Taylor & Francis
Taylor & Francis Group

Check for updates

Photo-assisted electrochemical degradation of polychlorinated biphenyls with boron-doped diamond electrodes

Rubén F. Gutiérrez-Hernández [a,b], Ricardo Bello-Mendoza [b,c], Aracely Hernández-Ramírez [d], Edi A. Malo [b] and Hugo A. Nájera-Aguilar [e]

aDepartamento de Ingeniería Química y Bioquímica, Instituto Tecnológico de Tapachula, Tapachula, Mexico; bEl Colegio de la Frontera Sur, Tapachula, Mexico; cDepartment of Civil and Natural Resources Engineering, University of Canterbury, Christchurch, New Zealand; dFacultad de Ciencias Químicas, Universidad Autónoma de Nuevo León, Monterrey, Mexico; eEscuela de Ingeniería Ambiental, Universidad de Ciencias y Artes de Chiapas, Tuxtla Gutiérrez, Mexico

ABSTRACT

The capacity of the photo electro-Fenton (PEF) process to degrade a mixture of seven polychlorinated biphenyl (PCB) congeners was studied. Boron-doped diamond (BDD) sheets were used as anode and cathode in the experimental electrolytic cell that contained Na_2SO_4 0.05 M at pH 3 as supporting electrolyte for the electro generation of H_2O_2 at the cathode. The effects of UV light intensity (254 and 365 nm), current density (8, 16 and 24 mA cm^{-2}) and ferrous ion dosage (0.1, 0.2 and 0.3 mM) on PCB ($C_0 = 50$ μg L^{-1}) degradation were evaluated. The highest level of PCB degradation (97%) was achieved with 16 mA cm^{-2} of current density, 0.1 mM of ferrous ion and UV light at 365 nm as irradiation source after 6 h of reaction. PCB28, PCB52 and PCB101 were not detected after 0.5, 1.5 and 3 h of reaction, respectively. The degradation of PCB138, PCB153, PCB180 and PCB209 was also high (>95%). The PEF system outperformed other oxidation processes (electro-Fenton, anodic oxidation, Fenton, photo-Fenton and UV photolysis) in terms of reaction rate and degradation efficiency. These results demonstrate for the first time the degradation of PCB209, the most highly chlorinated PCB congener, by an advanced electrochemical oxidation process.

1. Introduction

Polychlorinated biphenyls (PCBs) are known for their high toxicity, low biodegradability, for being bioaccumulative and for their potential to be transported over long distances. Due to these characteristics, PCBs have been included in the list of the 12 key persistent organic pollutants by the Stockholm convention [1]. The PCBs family consists of 209 congeners, all of them described by the empirical formula $C_{12}H_{10-n}Cl_n$ ($n = 1$–10) but with different number and position of chlorine atoms in their molecule. It is estimated that during the time the PCBs were produced, 1.3–2 million tons of these compounds were discharged to the atmosphere [2]. By the end of the 1970s, most governments banned the production of PCBs. However, even today widespread environmental contamination persists as a result of accidental spills and leaks that occurred in the past due to improper transportation, storage and disposal of PCBs [3]. The environmental presence of PCBs still represents a serious risk to both the environment and the human health (e.g. it is a risk factor for cancer and genetic mutations) [4]. For this reason, a large number of studies aimed at solving this pollution problem has been reported [1,5–7]. The degradation of PCBs has been studied using various chemical and biological processes such as incineration [8], biodegradation with fungi and bacteria [9,10], radiolytic degradation using Co^{60} as a source of γ rays [11], as well as some advanced oxidation processes (AOPs) [5,12]. However, there are still some limitations in the application of these methods. For example, the incineration of PCBs can produce undesirable products such as dioxins and furanes [8,13], which are more toxic than the PCBs themselves. Biological processes, despite being widely investigated, have high specificity [14], and, particularly, treatment times that can be as long as several months [15]. Meanwhile, most of the AOPs that have been studied had been able to degrade only PCBs with a low number of chlorine atoms in their molecule (mono, di-, tri-, tetra-, penta- or hexa-chlorinated) [1,5,16,17]. The AOPs most extensively studied in the degradation of PCBs are the Fenton (F) and the photo-Fenton (PF) systems. With these processes, it has been possible to significantly reduce treatment times from a length of months to days.

CONTACT Ricardo Bello-Mendoza ✉ ricardo.bellomendoza@canterbury.ac.nz 🖃 Department of Civil and Natural Resources Engineering, University of Canterbury, Private Bag 4800, Christchurch 8140, New Zealand

In recent years, the traditional set of AOPs has been extended to include novel electrochemical processes such as electro-Fenton (EF), photo electro-Fenton (PEF) and anodic oxidation (AO) systems, among others. The improvements brought about by these systems are due to the fact that they accomplish a continuous and *in situ* production of the precursor species of the degradation process. This way, the electrochemical advanced oxidation processes (EAOP) can achieve high degradation efficiencies on a broad spectrum of contaminating molecules. For example, these processes have been successfully applied to the degradation of pesticides [18–20], pigments and dyes [21,22], and various emerging contaminants such as pharmaceutical [23–25] and personal care products [26,27], among other molecules. In EAOPs, the electrode material plays an important role in the efficiency of degradation and different alternatives have been used including Pt electrodes, stainless steel, carbonaceous materials, Ag and boron-doped diamond (BDD) electrodes. Among the main advantages of BDD are its low capacitance, extreme electrochemical stability and, especially, its wide range of electrochemical potential in non-aqueous and aqueous media [23]. Furthermore, the high potential of such electrodes enables the production of larger amounts of $\cdot OH$ and consequently higher rates and degradation efficiencies. Considering the above, the coupling of the PEF system and BDD electrodes, as both anode and cathode, offers a promising alternative for treating chemically stable molecules such as highly chlorinated PCB congeners. The objective of this study was to evaluate the degradation of a mixture of seven PCB congeners (PCB28, PCB52, PCB101, PCB138, PCB153, PCB180 and PCB209) using the PEF system with BDD electrodes.

2. Materials and methods

2.1. Reagents

The mixture of standard grade PCBs (PCB28, PCB52, PCB101, PCB138, PCB153, PCB180 and PCB209, 1×10^4 µg L^{-1} of each one), Na_2SO_4 and H_2SO_4, both analytical reagent grade, and hexane and methanol, both HPLC grade, were obtained from Sigma-Aldrich. Analytical reagent grade $FeSO_4 \cdot 7H_2O$ and H_2O_2 were supplied by J. T. Baker. Distilled and deionised water was used in the preparation of all aqueous solutions.

2.2. Electrochemical system

The experiments were conducted in an undivided electrolytic cell of 50 mL working volume, filled with Na_2SO_4 0.05 M at pH 3 as supporting electrolyte. This pH value was used since many studies have reported that the optimum pH of the Fenton process is around 3 [28,29]. This is because iron species begin to precipitate as ferric hydroxides at higher pH values and form stable complexes with H_2O_2 at lower pH values, leading to deactivation of the catalyst. BDD electrodes (25 × 50 mm bipolar/Si 1 mm; Adamant Technologies, Switzerland), positioned in parallel with 2 cm spacing, were used as anode and cathode. Before starting the oxidation process, the reaction medium was saturated with oxygen by bubbling air at a flow of 300 mL min^{-1} for 45 min. Following this, electric current was induced into the system for an hour which enabled the electro production of hydrogen peroxide. Next, the reaction medium was spiked with the mixture of PCBs at a concentration of 50 µg L^{-1} for each of the seven congeners. Soon after, the oxidation process was initiated by adding Fe^{2+} and by irradiating the medium with UV light ($\lambda = 254$ and 365 nm). The degradation reaction was carried out for 6 h, and during this time, the agitation, temperature and air bubbling were maintained at constant values of 850 rpm, $25 \pm 2°C$ and 300 mL min^{-1}, respectively. The degradation of PCBs was monitored by analysing samples of the reaction medium collected every 90 min; this analysis was performed by gas chromatography. All glass materials used in the oxidation tests and chromatographic analyses were previously acid washed and heated at 450°C for 2 h.

2.3. Extraction of PCBs

PCBs were extracted from the aqueous phase using a liquid:liquid extraction method, with a 1:2 sample: solvent (hexane) ratio. This mixture was mixed vigorously for 10 min using a vortex. The recovered organic phase was mixed again with 0.075 g of Na_2SO_4 to remove moisture. Finally, the extract was stored until chromatographic analysis. The recovery percentages obtained with this method are presented in Table 1.

2.4. Chromatographic method

The analysis and quantification of PCB congeners was performed on a Clarus 500 gas chromatograph (Perkin Elmer, Massachusetts, USA) with an electron capture detector (GC-ECD). An MDS-5S glass capillary column (Supelco, Pasadena, USA) of 30 m long, 0.25-mm i.d. and 250-µm film was used. Samples (2 µL) were injected in split less mode. H_2 at 45.0 cm seg^{-1} was used as carrier gas. The temperatures of the injector and detector were set at 280°C and 350°C, respectively. The analysis was conducted using the following oven temperature

Table 1. Analytical method validation parameters.

Congener	R^2	% Recovery	RSD	LOD (μg L^{-1})	LOQ (μg L^{-1})
28	0.9512	97	2.54	0.1227	0.2971
52	0.9877	96	5.73	0.1060	0.2568
101	0.909	96	5.53	0.0493	0.1194
138	0.9787	98	1.75	0.0271	0.0657
153	0.9842	99	3.31	0.0252	0.0611
180	0.9787	98	1.6	0.0159	0.0386
209	0.9835	98	2.28	0.0248	0.0602

Note: RSD: relative standard deviation; LOD: limit of detection; LOQ: limit of quantitation.

program: 80°C for 1 min increased to 200°C with a ramp of 45°C min^{-1}; increased further to 250°C at 3°C min^{-1}, hold for 7 min. The validation of the chromatographic method was performed by determining the accuracy expressed as relative standard deviation (RSD), the linearity between the concentrations of the PCBs and their chromatographic response as denoted by R^2, the limit of quantitation (LOQ) and the limit of detection (LOD). The values obtained for these parameters are shown in Table 1.

2.5 . Analytical methods

The concentration of total iron and ferric ion (Fe^{3+}) was determined using the colorimetric method with phenanthroline, quantifying the complex formed at 510 nm [30]. The concentration of ferrous ion (Fe^{2+}) was calculated from the difference between the concentration of total iron and Fe^{3+}. The residual hydrogen peroxide was also monitored using a colorimetric method with titanium oxysulfate; the coloured complex was quantified at 406 nm. A UV/Vis spectrophotometer SQ-2800 (Cole Palmer) was used for these analyses.

2.6. Statistical analysis

Degradation tests followed a $2 \times 3 \times 3$ factorial design, where the UV light intensity (254 and 365 nm) was the first factor, the initial concentration of ferrous ion (0.1, 0.2 and 0.3 mM) was the second factor and the current density (8, 16 and 24 mA cm^{-2}) was the third factor. Statistical analysis of data was performed with Statisitica 7 (StatSoft, Inc.) software with a significance level of 5%.

3. Results and discussion

3.1. Degradation of PCBs by the PEF system

The ANOVA performed on the results of the PCB degradation tests by the PEF system (Table 2), showed the existence of significant differences among treatments. In this

test set, the highest percentage of degradation (97.5 ± 0.2% of the initial concentration of 350 μg ΣPCBs L^{-1}) was achieved when the system operated with 16 mA cm^{-2} of current density, 0.1 mM of Fe^{2+} and UV light at 365 nm (Figure 1). These results can be explained by the way reactions occur in the PEF system. The PEF process is initiated with the continuous production of H$_2$O$_2$ by the reduction of dissolved oxygen via two electrons (Equation (1)), which then reacts with the added Fe^{2+} to generate ·OH radicals (Equation (2)). Equations (1) and (2) show that as the current intensity increases, there is a higher generation of the oxidising species ·OH and, consequently, an increased degradation efficiency due to more ·OH being available to react with the saturated and aromatic organic compounds (Equations (3) and (4), respectively) [31]. However, it can also be expected that once certain concentrations of Fe^{2+} and H$_2$O$_2$ are reached, the degradation efficiency would start to decline [31,32]. This happens due to the occurrence of collateral reactions that compete for ·OH radicals. Reactions shown in Equations (5) and (6) are among the competitive reactions that contribute the most to diminished pollutant degradation efficiency. This system behaviour was observed in this study. Degradation efficiency showed a tendency to decrease with increased concentration of Fe^{+2} (Figure 1), which suggests that Fe^{+2} is not only reacting as shown in Equation (2) but also taking part of the reaction depicted by Equation (5). It can also be observed from Figure 1 that when current density increased from 8 to 16 mA cm^{-2}, the efficiency of PCB degradation also increased which can be explained by the electro generated H$_2$O$_2$ reacting mainly according to Equation (2). However, when current density increased from 16 to 24 mA cm^{-2}, the degradation efficiency showed a decline probably due to a higher oxidation of H$_2$O$_2$ as more ·OH radicals become available (Equation (6)).

$$O_2 + 2H + 2e^- \rightarrow H_2O_2 , \tag{1}$$

$$H_2O_2 + Fe^{2+} + H^+ \rightarrow Fe^{3+} + {}^\bullet OH + H_2O, \tag{2}$$
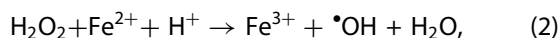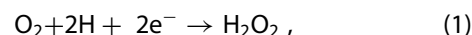
Table 2. ANOVA of oxidation tests results with PEF system.

Variation source	SS	DF	MS	F	p
Current density	128.544	2	64.27	5.74	.007
UV light intensity (wavelength)	3.479	1	3.48	0.31	.581
Fe^{2+} concentration	734.943	2	367.47	32.81	<.001
Current Density × Wavelength	137.705	2	68.85	6.15	.005
Current Density × Fe^{2+} Conc.	119.732	4	29.93	2.67	.047
Wavelength × Fe^{2+} Conc.	150.992	2	75.50	6.74	.003
Curr. Density × Wavelength × Fe^{2+} Conc.	214.100	4	53.53	4.78	.003
Residual	403.165	36	11.20		
Total	1893.661	53	35.71		

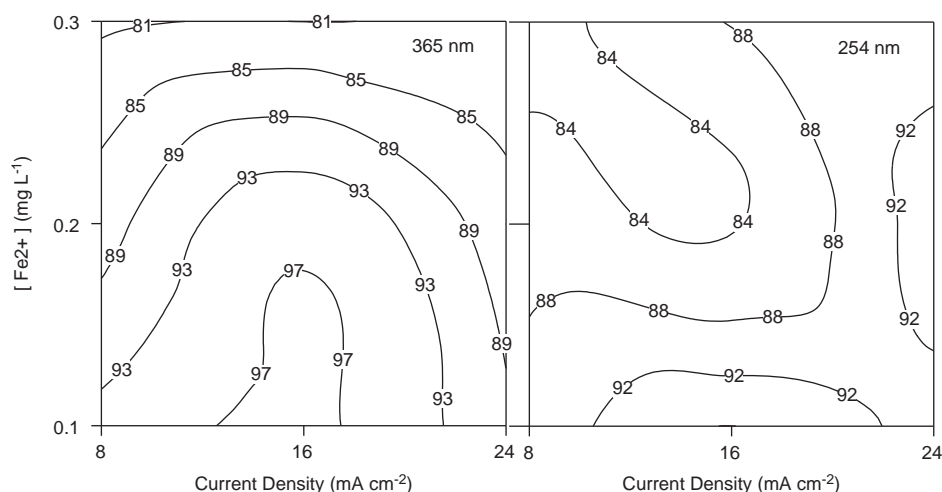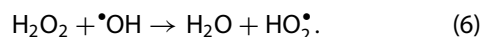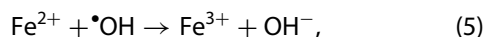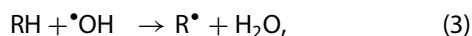Note: SS: sum of squares; DF: degrees of freedom; MS: mean square; F: F distribution; p: probability.

Figure 1. PCBs degradation efficiency (%) by the photoelectro-Fenton system ($C_0 = 350$ µg PCBs mixture L^{-1}).

$$RH + {}^{\bullet}OH \rightarrow R^{\bullet} + H_2O, \qquad (3)$$

$$ArH + {}^{\bullet}OH \rightarrow ArH({}^{\bullet}OH), \qquad (4)$$

$$Fe^{2+} + {}^{\bullet}OH \rightarrow Fe^{3+} + OH^{-}, \qquad (5)$$

$$H_2O_2 + {}^{\bullet}OH \rightarrow H_2O + HO_2^{\bullet}. \qquad (6)$$

On the other hand, the rate of degradation of PCB congeners by the PEF system was inversely proportional to the percentage of chlorination of each molecule (Figure 2). This behaviour has been reported in previous works where other PCB congeners have been degraded with different AOPs [1,5,16,33]. The concentration of the PCB28, PCB52 and PCB101 congeners was reduced below the LOD at 30, 180 and 270 min, respectively. Congeners with a higher number of chlorine atoms in their molecules (PCB138, PCB153, PCB180 and PCB209) were still detected in the residue obtained after the degradation process, although their concentrations were below 5% of the initial concentration. At the end of the oxidation process, there was a 96.3% reduction in the initial concentration of PCB209. The observed relationship between the efficiency of degradation and the percentage of chlorination of PCB congeners is due to the free ˙OH radicals reacting initially at unchlorinated positions, which decrease when the chlorination percentage increases, while the steric barrier increases [5,34]. This results in a great chemical stability which is characteristic of PCB molecules. Because of this, previous studies on
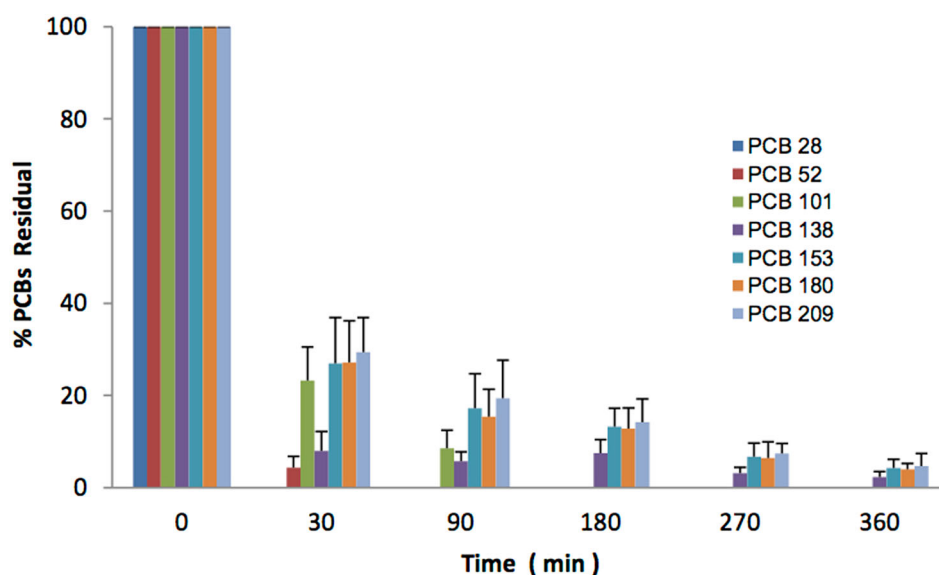

Figure 2. PCBs mixture degradation profile with the PEF system. The system was operated with a current density of 16 mA cm^{-2}, UV light at 365 nm and 0.1 mM of Fe^{2+}. The initial concentration of each congener was adjusted to 50 µg L^{-1}.

PCBs degradation using AOPs have focused on the oxidation of congeners with low percentages of chlorination [1,5]. This is the first time to the best of our knowledge that the degradation of the highly chlorinated and stable PCB209 congener by an EAOP is reported.

The strength of the PEF system is due to the fact that in this reaction medium various degradation processes such as H_2O_2/UV, H_2O_2/Fe^{2+} and AO, among others, occur simultaneously. In all these, the initial degradation step is the generation of ˙OH radical, and therefore, all degradation routes are conducted via free radicals. This EF system is enhanced when the reaction medium is irradiated with UV light because it produces the regeneration of Fe^{2+} from $Fe(OH)^{2+}$ photo reduction (Equation (7)) and from the photolysis of Fe^{3+} complexes with generated carboxylic acids (Equation (8)) [31]. This complete system represented by Equations (1)–(8) is known as PEF system.

$$Fe(OH)^{2+} + hv \rightarrow Fe^{2+} + {}^{\bullet}OH, \qquad (7)$$

$$Fe(OOCR)^{2+} + hv \rightarrow Fe^{2+} + CO_2 + R. \qquad (8)$$
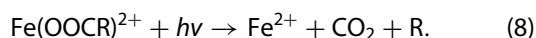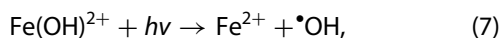
In the PEF system, H_2O_2 photolysis also occurs (Equation (9)). Likewise, water oxidation on BDD electrodes can produce large amounts of ˙OH radicals (Equation (10)), which remain adsorbed on the anode surface

($^{\bullet}OH_{ads}$). These ˙OH radicals are capable of reacting with the organic compounds until full mineralisation [35–37].

$$H_2O_2 + hv \rightarrow 2{}^{\bullet}OH, \qquad (9)$$

$$BDD + H_2O \rightarrow BDD({}^{\bullet}OH). \qquad (10)$$
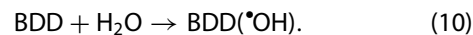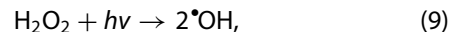
3.2. Concentration profiles during PEF treatment

The concentration profiles of the Fenton reagents and PCBs mixture during PEF treatment are presented in Figure 3. It can be seen that in the first 30 min of reaction, the high rate of consumption of both H_2O_2 and Fe^{2+} corresponds to the highest rate of degradation of the mixture of PCBs. After this initial period, the PCBs degradation rate decreases while the concentration of both H_2O_2 and Fe^{2+} is slightly recovered (see Equations (1), (7) and (8)). This is due to the fact that by lowering the concentration of PCBs (limiting reagent), the probability of collision and reaction of the reactants also decreases. Meanwhile, competing and recombination reactions are favoured, which is manifested in a decreasing rate of degradation of PCBs. On the other hand, the concentration profile of Fe^{3+} has an inverse behaviour than that of Fe^{2+}; that is to say, its concentration increases rapidly in the first 30 min and then a slight decrease and stabilisation is observed, which is justified by Equations (2), (7) and (8). Figure 3 shows that during
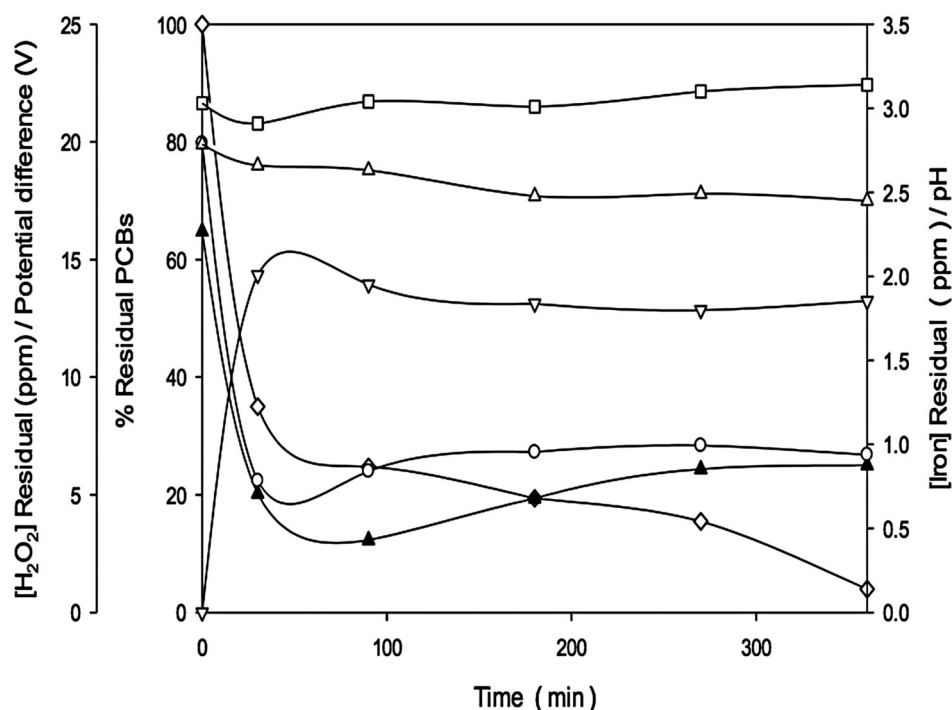

Figure 3. PEF system conditions along the degradation reactions. Initial concentration of the PCBs mixture was 350 µg L^{-1}. The system was operated with 16 mA cm^{-2}, 0.1 mM of Fe^{2+} and UV light at 365 nm. (□) pH, (△) Potential difference, (▽) Fe^{3+}, (○) Fe^{2+}, (▲) H$_2$O$_2$ and (◇) PCBs residual.

the degradation reaction, pH slightly increased; however, by the end of the reaction period, it is still within the range where Fenton type reactions are carried out optimally [38,39]. The monitoring of the potential difference showed that at the end of the reaction a potential of 17.5 V was held, which was 2.4 V below the initial value. This variation can be attributed to the generation of both negative and positive ions during the degradation process, which facilitate the electrical flow between the electrodes. One of these ions can be the Cl^- anion. The release of Cl^- ions during the photocatalytic treatment of PCB-contaminated soils has indeed been reported [40]. However, Prządo et al. [1] found no significant release of chloride ions from the degradation of PCBs by Fenton's reagent. If present in the electrochemical reaction medium, Cl^- anions may favour the formation of oxidising compounds such as HClO, responsible for indirect oxidation reactions [41]. They may also act as scavengers of hydroxyl radicals [42]. Moreover, the BDD anode can lead to the formation of higher oxidation states of chlorine, i.e. chlorite, chlorate and perchlorate [41].

3.3. UV light effect

The concentration profiles of H_2O_2, Fe^{2+} and Fe^{3+} in the reaction medium, both in the EF and in the PEF system, are presented in Figure 4. In both cases, the electro production of H_2O_2 was carried out under similar conditions

(16 mA cm^{-2}, 300 mL air min^{-1}); thus, the initial concentrations were approximately the same in both systems. However, it can be seen from Figure 4 that during the reaction period, H_2O_2 concentration was lower in the PEF than in the EF system. This could be the result of the photolysis of the H_2O_2 in the former system, as represented by Equation (9), which does not occur when the system is not photo-assisted. Therefore, the continuous generation (Equations (7) and (8)) and reaction (Equation (2)) of Fe^{2+} ion with H_2O_2 in the Fenton system, on the one side, and the photolysis of H_2O_2 (Equation (9)), on the other side, can explain the higher consumption of H_2O_2 in the PEF system. Furthermore, these same reactions (Equations (7) and (9)) explain an additional route generating ˙OH, which could increase the rate of degradation of PCBs in the photo-assisted system.

The behaviour of the Fe^{2+} ion is also observed in Figure 4. In the EF system, the Fe^{2+} concentration decreases during the reaction time, while in the PEF system a slight increase in its concentration is observed after the first 30 min of the reaction, which can be explained according to Equations (7) and (8).

3.4. Degradation process kinetics

The degradation of the PCBs mixture in the PEF system followed pseudo first-order kinetics (Table 3), which has also been observed when AOPs have been applied to the degradation of other molecules [18,43]. The
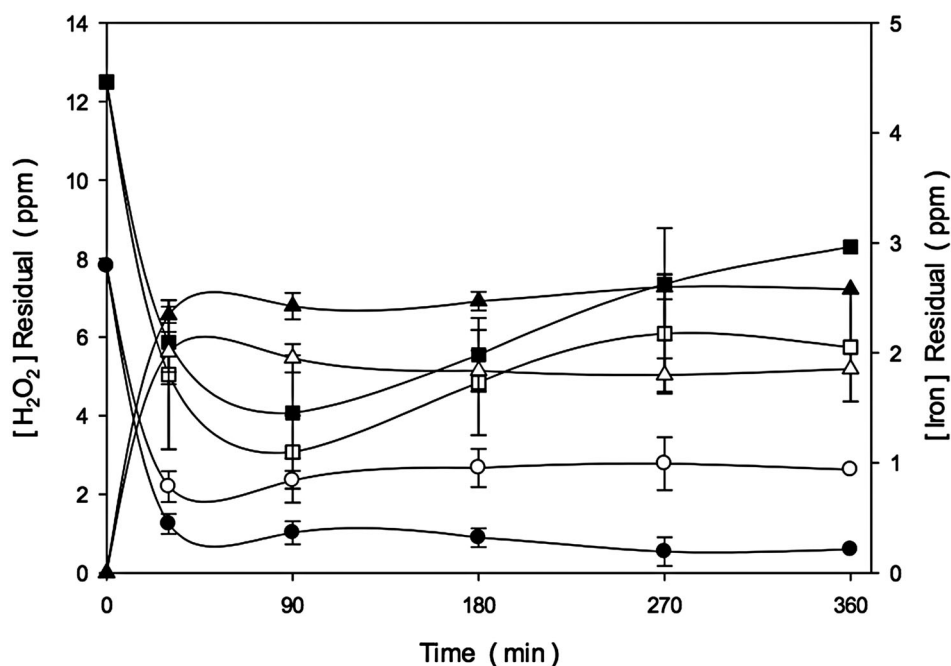

Figure 4. Concentration profiles of hydrogen peroxide and iron. (a) EF system: (■) H_2O_2, (●) Fe^{2+}, and (▲) Fe^{3+}. (b) PEF system: (□) H_2O_2, (○) Fe^{2+} and (△) Fe^{3+}.

Table 3. Apparent kinetic coefficients of the PEF system, using a current density of 16 mA cm^{-2}, 0.1 mM of Fe^{2+} and UV light at 365 nm.

Congener	First order		Pseudo first order	
	K (h^{-1})	R^2	K (L µg^{-1} h^{-1})	R^2
PCB28	–	–	–	–
PCB52	5.13	0.9673	0.2259	0.9022
PCB101	1.77	0.8807	0.0721	0.9992
PCB138	1.68	0.6737	0.1008	0.8384
PCB153	1.0695	0.7986	0.0305	0.9326
PCB180	1.1502	0.8385	0.0354	0.9692
PCB209	0.9958	0.7962	0.0262	0.9229
Mixture	1.137	0.7922	0.0191	0.9024

regression coefficients (R^2) presented in Table 3 confirm that the experimental data are well described by this type of reaction kinetics. As noted before, it has been reported on numerous occasions [1,5] the existence of an inverse relationship between the degree of chlorination and the degradability of the PCBs. The decrease in the values of the pseudo first-order kinetic coefficients (K) as the level of chlorination increases (Table 3) shows that the degradation of the PCB mixture generally fits the reported trend. However, there are two apparent exceptions. It can be seen that PCB101, with five chlorine atoms in its atomic structure, apparently degrades slower than PCB138, with six chlorine atoms. This can be the result of PCB101 being removed during the treatment process but also simultaneously produced, as an intermediary product, from the dechlorination of PCB

congeners with six or more chlorine atoms in their structure such as PCB153, PCB180 and PCB209. This would explain why after 30 min of reaction, the concentration of PCB101 is higher than that of PCB138 (Figure 2). A similar case happens with PCB153 and PCB180, although the concentration difference observed is much lower than in the case described above. This behaviour is consistent with previous reports [44].

3.5. Comparison of the PEF system with other AOPs

In order to compare the efficiency of the PEF system in degrading the PCBs mixture, additional tests were performed with other AOPs. The processes evaluated were F, EF, PF, AO, H_2O_2/UV and direct photolysis (DP) of PCBs. In the Fenton reaction, the initial concentration of H_2O_2 was 12.5 mg L^{-1} and 0.1 mM of Fe^{2+} ion. In AO, a current density of 16 mA cm^{-2} was applied, and in the case of photo-assisted systems UV light at 365 nm was used. These conditions were similar to those that allowed the highest PCBs removal in the PEF system. The degradation profile for each of the evaluated processes is presented in Figure 5. With the exception of DP, the degradation profile of the evaluated processes was adjusted to a pseudo first-order kinetic. The kinetics coefficient values obtained in each process (Table 4)
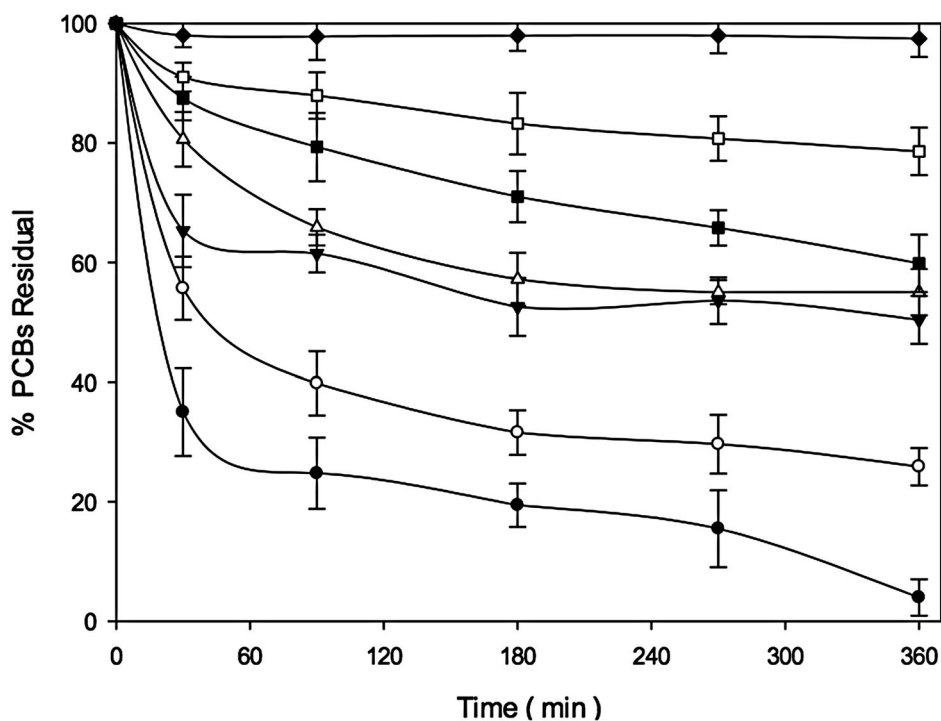

Figure 5. PCBs degradation profile with AOP: (●) PEF system, (○) EF system, (▼) PF system, (△) F system, (■) AO, (□) H_2O_2/UV and (◆) DP. The initial concentration of the mixture was adjusted to 350 µg L^{-1}.

Table 4. Kinetic coefficients (k) of pseudo first-order of each of the evaluated systems.

	System					
	PEF	EF	PF	F	AO	H_2O_2/UV
K (L μg^{-1} h^{-1})	0.0191	0.0097	0.0037	0.0024	0.0013	0.0008

Note: PEF: photo electro-Fenton; EF: electro-Fenton; PF: photo-Fenton; AO: anodic oxidation.

demonstrate that the PEF system presented the highest degradation rate ($k = 0.0191$ L μg^{-1} h^{-1}).

Among the evaluated processes, the DP presented the lowest degradation percentage (2.5%). With this system, only the PCB congeners with a low chlorination percentage were degraded [9]. This is because degradation is only promoted by the energy input from the UV light during the reaction. In the H_2O_2/UV system, the photolysis of both the PCBs mixture and H_2O_2 occurs (Equation (5)). The latter results in a second degradation route via free radicals. For this reason, the H_2O_2/UV system achieved a higher degradation percentage (21.5%) compared to DP. In the AO system, BDD sheets were used as electrodes since BDD is considered as the best material for a non-active anode, due to its weak interaction with the ˙OH generated according to Equation (10) [23]. With this system, a degradation percentage of 40.2% was achieved. The low degradation percentage is due to the fact that degradation in this process mainly depends on the probability of collision between a mobile species (i.e. PCB congeners) and the anode surface. This probability decreases as the concentration of mobile species is reduced.

The Fenton systems presented the highest removal percentages. The achieved degradation percentage was 45% with the F system, 49.6% with the PF system and 74.1% for the EF system. This is because in these systems, ˙OH radicals are dispersed in the reaction medium, which increases the probability of collision and reaction between them and the PCBs, consequently, the removal efficiency increases. The kinetic coefficients analysis (Table 4) shows that PEF, besides reaching the highest degradation percentage, also presented the highest degradation rate. The limiting factor in both F and PF systems is the availability of Fenton reagents which are depleted as reaction progress and hence the generation of ˙OH radicals also decreases. This limitation is not present in the PEF system where a continuous generation of H_2O_2 occurs, as in the EF. The advantage of the

PEF system is that the UV light energy supplied to the system results in an additional degradation pathway [45], and also causes the reduction of Fe^{3+} to Fe^{2+} which maintains high concentrations of the Fenton reagents. This explains why, compared to other AOPs, the PEF system achieved the highest percentage and rate of PCBs degradation.

The energy consumption (EC) for each process was calculated according to Equation (11) [18].

$$EC = \frac{VIt}{m_i - m_f},\qquad(11)$$

where EC is the energy consumption per unit mass of PCB removed, Kwh μg^{-1}; V is the potential difference between electrode, V; I is applied current, A; t is electrolysis time, hour; m_i is the mass of initial PCBs, μg; m_f is the mass of final PCBs, μg.

The EC for 300 min of electrolysis is shown in Table 5. In line with their higher efficiency in the removal of PCBs, the Fenton processes showed a lower EC when compared to the AO or the H_2O_2/UV systems. Among the Fenton processes, electro-Fenton was the most energy efficient in removing PCBs. The photo-assisted Fenton processes were less energy efficient which shows that the improvement in PCB degradation brought about by UV light irradiation comes at a high energy expense. Overall, the EC of the evaluated systems was much higher than those reported for the 5-min degradation of a pesticide (6.71×10^{-9}–54.17×10^{-9} kWh μg^{-1} pesticide) [18]. This difference can be explained by the lower initial concentrations of the PCBs and their higher recalcitrance which required a much longer treatment time.

4. Conclusions

The PEF system, operated with a current density of 16 mA cm^{-2}, 0.1 mM of Fe^{2+} and UV light at 365 nm, efficiently degraded seven PCB congeners with an initial total concentration of 350 μg L^{-1}. With this system, it was possible to reduce the treatment time reported in previous studies from days to hours. It was also possible to degrade the most highly chlorinated congener (i.e. PCB209). This is the first report of PCB209 degradation by an EAOP. This system proved to be the most efficient for PCBs degradation compared to the AO and other types of Fenton systems evaluated.

Table 5. Energy consumption (EC) of each of the evaluated systems.

	System				
	PEF	EF	PF	AO	H_2O_2/UV
EC (kWh μg^{-1} PCBs)	14.6×10^{-5}	9.7×10^{-5}	13.8×10^{-5}	17.9×10^{-5}	32.0×10^{-5}

Note: PEF: photo electro-Fenton; EF: electro-Fenton; PF: photo-Fenton; AO: anodic oxidation.

Disclosure statement

Funding

ORCID

Rubén F. Gutiérrez-Hernández http://orcid.org/0000-0001-8642-9075
Ricardo Bello-Mendoza http://orcid.org/0000-0002-4596-9363
Aracely Hernández-Ramírez http://orcid.org/0000-0002-4267-157X
Edi A. Malo http://orcid.org/0000-0002-1697-0277
Hugo A. Nájera-Aguilar http://orcid.org/0000-0002-9337-8242

References

[1] Prządo D, Kafarski P, Steininger M. Studies on degradation of polychlorinated biphenyls by means of Fentoń's reagent. Pol J Environ Stud. 2007;6(16):881–887.

[2] Ockenden WA, Breivik K, Meijer SN, et al. The global re-cycling of persistent organic pollutants is strongly retarded by soils. Environ Pollut. 2003;121(1):75–80.

[3] Passatore L, Rossetti S, Juwarkar AA, et al. Phytoremediation and bioremediation of polychlorinated biphenyls (PCBs): state of knowledge and research perspectives. J Hazard Mater. 2014;278:189–202.

[4] Hunt G, Stegeman J, Robertson L. PCBs: exposures, effects, remediation, and regulation with special emphasis on PCBs in schools. Environ Sci Pollut Res. 2016;23:1971–1974.

[5] Quiroga JM, Riaza A, Manzano MA. Chemical degradation of PCB in the contaminated soils slurry: direct Fenton oxidation and desorption combined with the photo-Fenton process. J Environ Sci Heal A. 2009;44:1120–1126.

[6] Mercier A, Joulian C, Michel C, et al. Evaluation of three activated carbons for combined adsorption and biodegradation of PCBs in aquatic sediment. Water Res. 2014;59:304–315.

[7] Demirtepe H, Kjellerup B, Sowers K, et al. Evaluation of PCB dechlorination pathways in anaerobic sediment microcosms using an anaerobic dechlorination model. J Hazard Mater. 2015;296:120–127.

[8] Ikonomou MG, Sather P, Oh JE, et al. PCB levels and congener patterns from Korean municipal waste incinerator stack emissions. Chemosphere. 2002;49:205–216.

[9] Chun CL, Payne RB, Sowers KR, et al. Electrical stimulation of microbial PCB degradation in sediment. Water Res. 2013;47:141–152.

[10] Kjellerup BV, Naff C, Edwards SJ, et al. Effects of activated carbon on reductive dechlorination of PCBs by organohalide respiring bacteria indigenous to sediments. Water Res. 2014;52:1–10.

[11] Schmelling DC, Poster D, Chaychian M, et al. Degradation of polychlorinated biphenyls induced by ionizing radiation in aqueous Micellar solutions. Environ Sci Technol. 1998;32:270–275.

[12] Zhang G, Hua I. Cavitation chemistry of polychlorinated biphenyls: decomposition mechanisms and rates. Environ Sci Technol. 2000;34:1529–1534.

[13] Shaub WM, Tsang W. Dioxin formation in incinerators. Environ Sci Technol. 1983;17:721–730.

[14] Pieper DH. Aerobic degradation of polychlorinated biphenyls. Appl Microbiol Biotechnol. 2005;67:170–191.

[15] Singer AC, Gilbert ES, Luepromchai E, et al. Bioremediation of polychlorinated biphenyl-contaminated soil using carvone and surfactant-grown bacteria. Appl Microbiol Biotechnol. 2000;54(6):838–843.

[16] Dercová K, Vrana B, Tandlich R, et al. Fenton's type reaction and chemical pretreatment of PCBs. Chemosphere. 1999;39:2621–2628.

[17] DeVor R, Carvalho-Knighton K, Aitken B, et al. Dechlorination comparison of mono-substituted PCBs with Mg/Pd in different solvent systems. Chemosphere. 2008;73:896–900.

[18] Yatmaz C, Uzman Y. Degradation of pesticide monochrotophos from aqueous solutions by electrochemical method. Int J Electrochem Sci. 2009;4:614–626.

[19] Navarro S, Fenoll J, Vela N, et al. Removal of ten pesticides from leaching water at pilot plant scale by photo-Fenton treatment. Chem Eng J. 2011;167:42–49.

[20] Cao M, Wang L, Wang L, et al. Remediation of DDTs contaminated soil in a novel Fenton-like system with zero-valent iron. Chemosphere. 2013;90:2303–2308.

[21] Sennaoui A, Sakr F, Dinne M, et al. Degradation of zenative yellow BF3R dye by the Fenton process. J Mater Environ Sci. 2014;5(5):1406–1411.

[22] Zuorro A, Lavecchia R. Evaluation of UV/H_2O_2 advanced oxidation process (AOP) for the degradation of diazo dye Reactive Green 19 in aqueous solution. Desalin Water Treat. 2014;52:1571–1577.

[23] Domínguez JR, González T, Palo P, et al. Anodic oxidation of ketoprofen on boron-doped diamond (BDD) electrodes. Role of operative parameters. Chem Eng J. 2010;162(3):1012–1018.

[24] Muruganantham M, Latha SS, Bhaskar G, et al. Anodic oxidation of ketoprofen – an anti-inflammatory drug using boron doped diamond and platinum electrodes. J Hazard Mater. 2010;180:753–758.

[25] De la Cruz N, Esquius L, Grandjean D, et al. Degradation of emergent contaminants by UV, UV/H_2O_2 and neutral photo-Fenton at pilot scale in a domestic wastewater treatment plant. Water Res. 2013;47(15):5836–5845.

[26] Jiang JQ, Zhou Z, Sharma VK. Occurrence, transportation, monitoring and treatment of emerging micro-pollutants in waste water- A review from global views. Microchem J. 2013;110:292–300.

[27] Borikar D, Mohseni M, Jasim S. Evaluation and comparison of conventional and advanced oxidation processes for the removal of PPCPs and EDCs and their effect on THM-formation potentials. Ozone Sci Eng. 2015;37:154–169.

[28] Nidheesh PV, Gandhimathi R. Trends in electro-Fenton process for water and wastewater treatment: an overview. Desalination. 2012;299:1–15.

[29] Wei J, Song Y, Tu X, et al. Pre-treatment of dry-spun acrylic fiber manufacturing wastewater by Fenton process: optimization, kinetics and mechanisms. Chem Eng J. 2013;218:319–326.

[30] APHA. Standard methods for the examination of water and wastewater. 18th ed. Washington (DC): American Public Health Association; 1992.

[31] Brillas E, Garrido JA, Rodriguez RM, et al. Wastewater by electrochemical oxidation processes using BDD anode and electrogenerated H_2O_2 with Fe(II) and UV light as catalysts. Port Electrochim Acta. 2008;26:15–46.

[32] Gutiérrez RF, Santiesteban A, Cruz-López L, et al. Removal of chlorothalonil, methyl parathion and methamidophos from water by the Fenton reaction. Environ Tech. 2007;28:267–272.

[33] Riaza-Frutos A, Quiroga JM, Manzano MA. Remediation of contaminated soils with PCBs using an integrated treatment: desorption and oxidation. J Environ Eng. 2007;133:541–547.

[34] Sediak DL, Andrew WA. Aqueous-phase oxidation of polychlorinated biphenyls by Hidroxyl radicals. Environ Sci Technol. 1991;25:1419–1427.

[35] Michaud PA, Panizza M, Ouattara L, et al. Electrochemical oxidation of water on synthetic boron-doped diamond thin film Anodes. J Appl Electrochem. 2003;33:151–154.

[36] Martínez-Huitle CA, Ferro S. Electrochemical oxidation of organic pollutants for the wastewater treatment: direct and indirect processes. Chem Soc Rev. 2006;35:1324–1340.

[37] Garrido JA, Brillas E, Cabot PL, et al. Mineralization of drugs in aqueous medium by advanced oxidation processes. Port Electrochim Acta. 2007;25:19–41.

[38] Mackuĭak T, Takáčová A, Gál M, et al. PVC degradation by Fenton reaction and biological decomposition. Polym Degrad Stab. 2015;120:226–231.

[39] Ramteke LP, Gogate PR. Treatment of toluene, benzene, naphthalene and xylene (BTNXs) containing wastewater using improved biological oxidation with pretreatment using Fenton/ultrasound based processes. J Ind Eng Chem. 2015;28:247–260.

[40] Occulti F, Roda GC, Berselli S, et al. Sustainable decontamination of an actual-site aged PCB-polluted soil through a biosurfactant-based washing followed by a photocatalytic treatment. Biotech Bioeng. 2008;99(6):1525–1534.

[41] Cabeza A, Urtiaga AM, Ortiz I. Electrochemical treatment of landfill leachates using a boron-doped diamond anode. Ind Eng Chem Res. 2007;46(5):1439–1446.

[42] Pignatelo JJ, Oliveros E, MacKay A. Advanced oxidation processes for organic contaminant destruction based on the Fenton reaction and related chemistry. Crit Rev Environ Sci Technol. 2006;36:1–84.

[43] Aaron JJ, Oturan MA. New photochemical and electrochemical methods for the degradation of pesticides in aqueous media-environmental applications. Turk J Chem. 2001;25:509–520.

[44] Yao Y, Kakimoto K, Ogawa HI, et al. Photodechlorination pathways of non-ortho substituted PCBs by ultraviolet irradiation in alkaline 2-propanol. Bull Environ Contam Toxicol. 1997;59:238–245.

[45] Dasary SSR, Saloni J, Fletcher A, et al. Photodegradation of selected PCBs in the presence of nano-TiO_2 as catalyst and H_2O_2 as an oxidant. Int J Environ Res Public Health. 2010;7:3987–4001.